HHS Public Access

Author manuscript

J Control Release. Author manuscript; available in PMC 2019 June 17.

Published in final edited form as:

J Control Release. 2018 September 10; 285: 35–45. doi:10.1016/j.jconrel.2018.07.001.

PEGylated enhanced cell penetrating peptide nanoparticles for lung gene therapy

Gizem Osman[a], **Jason Rodriguez**[b], **Sze Yan Chan**[a], **Jane Chisholm**[b,c], **Gregg Duncan**[b,d], **Namho Kim**[b,c], **Amanda L. Tatler**[e], **Kevin M. Shakesheff**[a], **Justin Hanes**[b,c,f], **Jung Soo Suk**[b,c,f,**], **James E. Dixon**[a,*]

[a]Wolfson Centre for Stem Cells, Tissue Engineering, and Modelling (STEM), Centre of Biomolecular Sciences, School of Pharmacy, University of Nottingham, Nottingham NG7 2RD, UK

[b]The Centre for Nanomedicine, Johns Hopkins University School of Medicine, Baltimore, MD 21231, USA

[c]Department of Chemical & Biomolecular Engineering, Johns Hopkins University, Baltimore, MD 21218, USA

[d]Fischell Department of Bioengineering, University of Maryland, College Park, MD 20742, USA

[e]Nottingham NIHR Biomedical Research Centre, Division of Respiratory Medicine, University of Nottingham, Nottingham University Hospitals NHS Trust, City Hospital, Nottingham NG5 1PB, UK

[f]Department of Ophthalmology, Johns Hopkins University School of Medicine, Baltimore, MD 21231, USA

Abstract

The lung remains an attractive target for the gene therapy of monogenetic diseases such as cystic fibrosis (CF). Despite over 27 clinical trials, there are still very few gene therapy vectors that have shown any improvement in lung function; highlighting the need to develop formulations with improved gene transfer potency and the desirable physiochemical characteristics for efficacious therapy. Herein, we introduce a novel cell penetrating peptide (CPP)-based non-viral vector that utilises glycosaminoglycan (GAG)-binding enhanced transduction (GET) for highly efficient gene transfer. GET peptides couple directly with DNA through electrostatic interactions to form nanoparticles (NPs). In order to adapt the GET peptide for efficient in vivo delivery, we engineered PEGylated versions of the peptide and employed a strategy to form DNA NPs with different densities of PEG coatings. We were able to identify candidate formulations (PEGylation rates ≥ 40%) that shielded the positively charged surface of particles, maintained

*Correspondence to: J. E. Dixon, Wolfson Centre for Stem Cells, Tissue Engineering, and Modelling (STEM), Centre for Biomolecular Sciences, University of Nottingham, University Park, Nottingham NG7 2RD, UK. james.dixon@nottingham.ac.uk (J.E. Dixon). **Correspondence to: J. S. Suk, The Centre for Nanomedicine, Department of Ophthalmology, Johns Hopkins University School of Medicine, Baltimore, MD 2123, USA. jsuk@jhmi.edu (J.S. Suk).

Competing financial interests

The authors declare no competing financial interests.

Appendix A. Supplementary data

Supplementary data to this article can be found online at https://doi.org/10.1016/j.jconrel.2018.07.001.

colloidal stability in bronchoalveolar lavage fluid (BALF) and retained gene transfer activity in human bronchial epithelial cell lines and precision cut lung slices (PCLS) in vitro. Using multiple particle tracking (MPT) technology, we demonstrated that PEG-GET complexes were able to navigate the mucus mesh and diffuse rapidly through patient CF sputum samples ex vivo. When tested in mouse lung models in vivo, PEGylated particles demonstrated superior biodistribution, improved safety profiles and efficient gene transfer of a reporter luciferase plasmid compared to non-PEGylated complexes. Furthermore, gene expression was significantly enhanced in comparison to polyethylenimine (PEI), a non-viral gene carrier that has been widely tested in pre-clinical settings. This work describes an innovative approach that combines novel GET peptides for enhanced transfection with a tuneable PEG coating for efficacious lung gene therapy.

Keywords

Glycosaminoglycan-binding enhanced; transduction (GET); Lung; Transfection; Gene therapy; Cell-penetrating peptide (CPP); Plasmid DNA (pDNA)

1. Introduction

Cystic fibrosis (CF) is an inherited incurable disease that affects > 70,000 patients globally and is caused by an underlying genetic mutation in the CF *transmembrane conductance regulator (CFTR)* gene [1]. Although CF is a multisystem disease that affects many organs, about 90% of patient death is due to respiratory failure, making the lungs a critical target for gene therapy of the disease [2]. Over 1990 different mutations of the *CFTR* gene have been reported [3]. The majority of mutations (including the most common F508del affecting 70% of CF patients) cause the production of defective CFTR proteins that are no longer able to regulate cyclic adenosine monophosphate (cAMP)-dependent chloride secretion, bicarbonate secretion and epithelial sodium channels (ENaCs). Eventually this leads to incorrect transport of ions, mucus stasis/plugging, chronic lung infections and pulmonary failure [4].

Since the first human CF gene therapy trial in 1989, 27 clinical trials have been carried out by viral (e.g. adenovirus and adeno-associated virus; AAV) and non-viral (e.g. lipid and cationic polymer) vectors [5–8]. The majority of viral technologies cannot penetrate mucosal secretions leading to poor efficacy and/or have safety concerns inhibiting their clinical adoption [9]. In 2015, the outcome of the first-in-man phase 2b trial of a non-viral gene therapy for CF using a cationic liposome-based vector, termed GL67A, was published by the UK Cystic Fibrosis Gene Therapy Consortium (UKCFGTC) [10]. This was a one year trial designed to assess clinical efficacy following monthly repeated delivery of plasmid (p)DNA/GL67A in 136 patients with CF. The *CFTR* gene used in the trial was specifically engineered to be cytosine-phosphate-guanidine (CpG) free and contain a human elongation factor 1 alpha (EF1A1) promoter for reduced inflammatory response and prolonged gene expression, respectively [11]. Inhaling the liposomal vector was safe over a 1 year period and had a marginal beneficial effect on lung function. Despite the limited and variable efficacy, this was the first clinical demonstration showing that repeated administration of non-viral gene carriers is a feasible and well-tolerated approach for the treatment of CF.

Developing successful airway gene therapy is complex as gene transfer agents must penetrate lung mucus and reach the airway epithelium prior to removal from the lung by mucociliary clearance (MCC) [12]. This navigation is even more challenging in CF lungs due to pathological alteration of mucus properties that makes this barrier even harder to penetrate [13]. CF sputum is a highly dense meshwork composed of mucin fibres, possessing negatively charged and hydrophobic domains, and other adhesive macromolecules such as DNA fragments released from bacteria and endogenous cells [14]. As a consequence, particle diffusion is largely impeded within the mucus gel by steric obstruction and/or mucoadhesive interactions with sputum components. In particular, conventional non-viral gene vectors formulated with cationic materials possess positively charged surfaces and thus are readily trapped by negatively charged mucus via electrostatic interactions [15]. Furthermore, charged particles rapidly aggregate in physiological ionic environments, leading to entrapment within the mucus gel via steric obstruction [16]. It has previously been demonstrated that the modification of particle surfaces with a dense layer of poly(ethylene glycol) (PEG) inhibits particle aggregation as well as mucoadhesion, thereby leading to efficient mucus penetration of nanoparticles (NPs) [17, 18]. Importantly, due to their ability to penetrate airway mucus, PEGylated DNA NPs have been shown to provide widespread airway distribution, prolonged lung retention and ultimately a high-level transgene expression following inhalation [19–21].

The work presented here is based on novel modified cell penetrating peptide (CPP)-based gene vectors. Glycosaminoglycan (GAG)-binding enhanced transduction (GET) peptides are multi-domain sequences comprising of a heparan sulfate (HS) cell targeting sequence fused to a CPP for improved membrane association and synergistically enhanced intracellular delivery of therapeutic cargoes [22]. We have previously described GET peptides for improved delivery of a self-reporting cargo (monomeric red fluorescent protein; mRFP) in difficult-to-transduce cell types including mesenchymal stem cells (MSCs), human embryonic stem cells (hESCs) and human induced pluripotent stem cells (hiPSCs). The GET-system has been utilised for a wide variety of applications from the spatio-temporal control of cell programming in hydrogel matrices to the delivery of runt-related transcription factor 2 (RUNX2) for osteogenesis of MSCs [23, 24]. Furthermore, GET-mRFP proteins have retained activity when encapsulated into poly(DL-lactic acid-*co*-glycolic acid) (PLGA) microparticles for controlled release and sustained delivery to cells over extended periods of time [25].

The initial transfection peptide we generated (P21 LK15 8R; PLR) was the prototypical example used for nucleotide transfection; mediating delivery of DNA- (plasmids) and RNA-based (siRNA, mRNA) macromolecules into cells [22]. When tested against commercial transfection reagent Lipofectamine 2000, PLR demonstrated comparable transfection efficiency albeit requiring a higher DNA dose to produce the same effect. We also tested other peptide versions containing different HS-binding sequences, one such was derived from fibroblast growth factor 2 (FGF2) (termed FGF2B) [26]. FGF2B (TYRSRKYTSWYVALKR) is a short 16-residue peptide that shows no significant cell penetrating properties by itself, however when coupled to a CPP it demonstrated up to two orders of magnitude enhanced delivery of recombinant proteins into a wide variety of cell types compared to an unmodified CPP [22]. Herein we describe GET transfection

peptide FGF2B LK15 8R (FLR) for superior DNA complexation, enhanced gene delivery and highly efficient transfection of cells in vitro. We prepared various formulations of PEG DNA NPs, each made-up of different molar ratios of PEGylated to non-PEGylated FLR peptide as a strategy to incorporate a controlled density of PEG on the particle surface. We hypothesized that by using this strategy we could engineer PEGylated complexes with tuneable properties that were stable in biological fluids, retained enhanced transfection activity and could rapidly penetrate human CF sputum. Candidate formulations were tested for their ability to demonstrate efficient, widespread and safe transgene expression in healthy mouse lung models in vivo.

2. Results and discussion

2.1. DNA NP formation and stability profiles

The gene transfer potential of FGF2B had not yet been evaluated. To test this we designed the FLR peptide, including the amphipathic sequence LK15 (L) to improve the DNA condensation ability and intracellular trafficking of the peptide [27, 28] along with octa-arginine (8R) as the CPP (Fig. 1A). Initially, we assessed the DNA complexation ability of FLR and its components by the YO-PRO-1 assay; a fluorescence-based competition assay conventionally used to determine strength of complexation between DNA and non-viral gene vector materials via quenching of fluorescence [29, 30]. FLR was capable of condensing DNA through electrostatic interactions between the positively charged amines of the peptide and the negatively charged phosphate groups of the DNA, eliminating the need for complex chemical conjugation and deconjugation steps. Complexation was rapid, with the full effect on fluorescence quenching observed within 30 s. We compared peptide variants 8R (R), LK15 8R (LR) and FLR (peptide sequences shown in Table S1). All the tested peptides demonstrated DNA condensing activity, however those containing LK15 required the lowest charge ratio (CR) to achieve complete removal of fluorescence (Fig. 1B). The LR and FLR peptides were able to complex 98.5 ± 0.1% and 96.2 ± 0.5% of DNA at CR3, respectively. However the unmodified CPP (R alone) was only able to complex 90.3 ± 0.5% of the DNA at the highest tested CR. The hydrodynamic size and zeta potential of the DNA NPs were measured in water and 10 mM NaCl at pH 7.0, respectively (Fig. 1C). At CR1 the hydrodynamic size was 267 ± 6 nm and zeta potential was −24 ± 1 mV indicating that there was insufficient peptide present to condense the DNA. FLR was able to form positively charged, small and stable NPs at CR ≥ 2. The polydispersity index (PDI) of the DNA NPs was about 0.2, which indicated relatively uniform size distribution of the complexes devoid of large aggregates or sedimentation.

We next explored the possibility of functionalising DNA NPs with PEG chains. We introduced an N-terminal cysteine to the FLR peptide. 5 kDa PEG maleimide was covalently conjugated to the peptide through formation of a stable thioether linkage with the thiol group of the cysteine residue [31]. We hypothesized that the cationic peptide would compact the DNA in the centre of the particles and the PEG chains would orient themselves to form a layer on the particle surface. Thereby, at different PEGylation rates we could achieve different densities of PEG coatings on the DNA NP surface (Fig. 2A). A blend of different molar ratios of non-PEGylated and PEGylated FLR peptides were mixed with DNA at CR3

to form particles at different PEGylation rates. To assess the surface characteristics of the DNA complexes, their hydrodynamic diameter and zeta potential were measured. The sizes of the DNA NPs at all tested PEGylation rates were between 97 and 107 nm, indicating that inclusion of PEGylated peptides did not undermine the ability of the peptides to condense DNA into compact NPs (Fig. 2B). DNA complexes formulated with non-PEGylated peptides exhibited a high positive charge of 21 ± 1 mV. The cationic charge gradually dropped when incrementing fractions of PEGylated peptides were used, down to a near neutral surface charge observed for DNA complexes made entirely with PEGylated peptides. This finding signifies that particle surface shielding can be achieved by precisely controlling the proportions of PEGylated peptides.

Next, we investigated whether PEGylation could shield DNA NPs from enzymatic digestion of DNA payloads and from particle aggregation in a physiologically relevant biological fluid. To assess the ability of FLR peptides to provide efficient protection against nuclease activity, DNA complexes were incubated with increasing concentrations of nuclease (DNase I) and analysed using a gel shift assay. Naked pDNA was digested by DNase I at all tested concentrations (Fig. 2C). In comparison, DNA NPs made up with non-PEGylated or PEGylated FLR peptides improved DNA protection following degradative challenge. To investigate whether PEGylation prevented DNA NPs from aggregation in a physiologically relevant fluid, we incubated complexes in water or bronchoalveolar lavage fluid (BALF). BALF, which is collected from lungs following a lavage procedure with phosphate-buffered saline (PBS), is made up of a mixture of epithelial lining fluid (ELF) and tissue-specific cells including immune cells, squamous epithelial cells and bronchial epithelial cells [32]. Proteomics of BALF has shown that it contains a dynamic and diverse protein composition that is representative of pulmonary airways [33]. Following incubation in BALF for 1 h, the hydrodynamic size of complexes was measured to determine whether they were able to retain colloidal stability; a physical state in which particles remain dispersed in a solution at equilibrium. Kinetically unstable particles coagulate and form aggregates. It is estimated that airway mucus has pore sizes of about 200 nm [34], therefore aggregates or large particles sized beyond this cut-off are unlikely to diffuse efficiently through the airway due to steric hindrance. The size of DNA NPs in water remained between 93 and 125 nm at all tested PEGylation rates (Fig. 2D). However, when incubated in BALF complexes of low PEGylation rates exhibited up to a 20-fold increase in particle diameter. Colloidal stability in BALF was achieved at ≥40% PEGylation where particle size was between 142 and 167 nm. Importantly, DNA NPs that are able to maintain a diameter of < 200 nm would have the best chance of navigating the mucus mesh and reaching airway epithelium [35].

2.2. Optimized transfection of DNA NPs in vitro

Following successful formation of DNA NPs, the gene transfer potency of the FLR vector was investigated in vitro. In this study, we compared the transfection efficiencies of GET peptides, FLR and PLR, in NIH3T3 cells via transfection of a reporter pDNA encoding green fluorescent protein (GFP) [22]. Cells were fixed 24 h post treatment to allow time for the transient expression of GFP to be captured and the percentage of transfected cells to be quantified by flow cytometry. We observed that the transfection efficiency of FLR was enhanced at CRs ≥ 3 where more cationic peptide component was present in the NPs

(Fig. S1). Both FLR and PLR peptides exhibited high transfection efficiency (60.9 ± 5.5% and 29.8 ± 7.8%, respectively). High PLR-mediated transfection requires higher pDNA dose than FLR as previously described [22]. LR peptides (lacking a HS targeting domain) exhibited lower transfection efficiency (12.5 ± 2.9%), highlighting the need for the full multi-functional peptide for superior transfection. The difference in transfection efficiency observed between GET peptides, FLR and PLR, is likely due to targeting of different cell surface HS-epitopes. We have previously confirmed that the distinct cell surface sulfation patterns displayed on the membrane affect the ability of the different HS binding sequence to interact with them [22]. When tested against a variety of leading commercial transfection reagents including Lipofectamine 2000 (lipid-based), Lipofectamine 3000 (lipid-based), JetPEI (polymer-based), TransIT-LT1 and FuGENE HD (both non-liposomal formulations composed of both lipid and protein components), we found that FLR was comparable to or outperformed the commercial systems by demonstrating both high efficiency (% GFP positive cells) and low cytotoxicity (Fig. S2).

Our next aim was to test the effect of PEGylation on uptake and transfection efficiency in a human bronchial epithelial cell line (BEAS2B-R1) using a luciferase reporter gene. PEG shields can greatly improve colloidal stability however this is often achieved at the expense of undermining the ability of cationic gene vectors to achieve efficient gene transfer [36]. This effect is presumably caused by the PEG chains that sterically hinder the interaction of the membrane-active particle core with the cell surface. The shielding effect of the PEG corona has also been reported to sterically inhibit the endosomal release of lipid and polymer-based gene vectors which are heavily reliant on endosomal escape strategies for high efficiency of transfection [37–39]. Conversely, once inside the cell, PEGylation has been shown to improve the diffusion of DNA NPs through the cytoplasm by reducing adhesive interaction with surrounding bio-components [40]. The PEG chains may also act to weaken the association between the gene carrier and DNA. Thereby, improving intracellular de-packaging, release and bioavailability of the gene [41]. GET peptides utilize HS-GAG binding ligands to enhance cell surface concentration, membrane association and in turn improve their translocation across the cellular membrane. Therefore, candidate PEG peptide formulations must be carefully selected to maintain a balance between their ability to overcome extracellular barriers and retain enhanced intracellular delivery of target genes. In agreement with previous reports, we found that increasing the PEGylation rate led to a gradual decrease in DNA uptake and transgene expression in comparison to non-PEGylated particles (Fig. 3). When compared to Lipofectamine 2000 and Lipofectamine 3000, we observed that 0%, 10%, 20% and 40% PEGylated FLR peptides exhibited significantly more efficient intracellular uptake. The transfection efficiency of non-PEGylated FLR peptides was comparable to Lipofectamine 2000, however Lipofectamine 3000 demonstrated the highest in vitro gene transfer. Interestingly, we found that BEAS2B-R1 cells were exceptionally sensitive to treatment via the commercial transfection reagents in comparison to NIH3T3 cell lines (Fig. S2B), with both Lipofectamine 2000 & 3000 significantly effecting cell viability.

Despite demonstrating promising in vitro efficiency in lung cell lines, there are still very few gene therapy vectors that have shown any improvement in lung function in vivo; highlighting the need to further evaluate gene transfer in models that retain or mimic native

tissue and cell types. Precision cut lung slices (PCLSs) utilize agarose to stabilise tissue before sectioning to create a tractable pre-clinically relevant lung assay which has previously been used for drugs testing and respiratory disease modelling [42, 43]. In order to examine efficiency and toxicity of gene therapy strategies directly in mouse lung tissues we treated PCLSs with PEGylated formulations, Lipofectamine 2000 or Lipofectamine 3000 (Fig. S3). We demonstrated that FLR peptides at a PEGylation rates ≥ 40% exhibited enhanced gene transfer of a reporter luciferase plasmid in comparison to the lipid-based commercial transfection reagents (with very poor efficiencies; 29 ± 14 RLU/mg and 24 ± 17 RLU/mg for Lipofectamine 2000 and 3000, respectively). In addition, we have shown that FLR peptides did not negatively affect the viability of tissues at any of the tested PEGylation rates. To this end, DNA NPs for in vivo applications should be determined based both on colloidal stability in a relevant physiological environment and ability to transfect cells. DNA NPs formulated with an inclusion of 40% PEGylated peptide were thus selected as good candidates for subsequent studies as they demonstrated the highest in vitro transfection activity among formulations and retained an acceptable colloidal stability in BALF (Fig. 2D).

2.3. Ex vivo NP tracking in human CF sputum samples

Next, we compared the ex vivo diffusion of 0%, 40% and 60% PEGylated particles through sputum samples freshly collected from CF patients. We compared 40% with 60% as examples of PEGylation quantities around the threshold at which transfection efficiency was affected. TEM images of PEGylated DNA complexes were suggestive of the formation of spherical compact particles (Fig. 4A). NP dimensions were in agreement with hydrodynamic size measurements. Multiple particle tracking (MTP) technology was used to analyze the diffusion of cyanine3 (Cy3) and/or cyanine5 (Cy5)-labelled DNA NPs [44]. The mean squared displacement (MSD) is a square of distance travelled by an individual particle at a given time interval (i.e. time scale), and thus the MSD is directly proportional to particle diffusion rates [9]. The representative trajectories of the tested formulations demonstrated that particles lacking the PEG component exhibited constrained movement in CF mucus in comparison to greater distances travelled by 40% and 60% PEG DNA NPs (Fig. 4B–C).

It has been reported that inhaled particles are cleared rapidly from the mucus of CF patients within the first hour [45]. Here, we defined particles capable of diffusing through sputum with MSD ≥ 1 μm^2 at a time scale of 1 s as “mucus penetrating” based on their diffusive trajectories; these particles are likely to have greater chances of reaching the epithelium covered by the airway mucus gel layer prior to being cleared from the lung via MCC. On average, median MSD values were greater for PEGylated DNA NPs compared to their non-PEGylated counterpart; however, the differences were not statistically significant presumably due to the highly heterogeneous nature of CF sputum (Fig. 4D). Nonetheless, ~30% of PEGylated DNA NPs (of 40% or 60% PEG) were categorized as mucus penetrating fractions, which is 6-fold greater than the fraction observed with non-PEGylated particles (i.e. ~5%), reaching statistically significant differences (Fig. 4E).

2.4. In vivo gene delivery in healthy mouse lung models

It is thought that successful treatment of lung diseases such as CF can be achieved by even low transgene expression in minimal numbers of cells (≤ 10% of cells) [46, 47]. We expected that PEGylated formulations with improved stability-profiles and mucus penetrating properties would provide more widespread gene delivery in the airways and alveolar region (parenchyma) compared to non-PEGylated particles in vivo. Although mucus is not abundant in the lung parenchyma, pulmonary surfactants produced by type II alveolar epithelial cells have similarly been shown to readily interact with naked cationic gene vectors resulting in de-stabilization and aggregation of DNA-gene carrier complexes [48, 49]. As 40% PEGylated NPs retain both transfection efficiency in vitro and stability ex vivo we compared this to non-PEGylated NPs by aerosolizing them into mouse lungs. To visualize the distribution of 0% and 40% PEGylated complexes in mouse lung models in vivo, DNA NPs containing Cy5-labelled DNA were intratracheally administered by an aerosol-generating microsprayer to the lungs of 6–8 week female BALB/c mice. Thirty minutes following administration, lungs were harvested and analysed by fluorescence microscopy. Non-PEGylated DNA NPs appeared to be sparsely distributed in the lumen, in contrast to the widespread and more uniform distribution observed with 40% PEG DNA NPs (Fig. 5A). Image-based quantification of fluorescence confirmed that PEGylated particles exhibited significantly greater coverage in both large airways (Fig. 5B) and the lung parenchyma (Fig. 5C).

Next, we sought to determine whether improved lung distribution by PEGylation translated to enhanced gene transfer in vivo of a luciferase-expressing plasmid. Luciferase is not a cell autonomous reporter and as such does not allow the quantification of the percentage of transfected cells. However Luciferase bioluminescence allows non-invasive quantitative transgene expression to be measured directly. Each mouse was treated with 10 μg of DNA carried by different delivery systems, including non-PEGylated FLR peptides, PEGylated FLR peptides or polyethylenimine (PEI). PEI is a non-viral polymer-based gene vector that has been widely explored for preclinical lung gene therapy studies [50] but previously been shown to be unable to efficiently penetrate CF sputum [19] similar to our observation with the non-PEGylated peptide in this study (Fig. 4). Mice treated with 40% PEG DNA complexes demonstrated significantly superior transgene expression compared to non-PEGylated DNA NPs and PEI DNA NPs (Fig. 6A). Despite their high in vitro transfection efficiency, DNA NPs based on non-PEGylated peptides failed to provide significantly improved in vivo gene transfer efficacy compared to the DNA only control, underscoring the importance of testing gene vectors in relevant in vivo conditions.

Following inhalation, gene vectors can be rapidly cleared by alveolar macrophages directly via opsonin-independent scavenger receptors or by opsonin-dependent mechanisms. Other immune cells, including neutrophils, are also recruited as part of the innate immune response. Opsonins (proteins present in serum) are adsorbed onto the surface of foreign particles [51]. Alveolar macrophages can easily recognize, engulf and destroy opsonized DNA NPs as well as triggering lung epithelial cell-mediated production of pro-inflammatory cytokines [52]. Pro-inflammatory cytokines, such as TNF-α and IL-1β, initiate the production of further inflammatory mediators which can eventually cause acute lung toxicity

by disrupting pulmonary endothelial cells and compromising epithelial integrity [53]. It is well documented that PEGylation can help improve the safety profile of DNA NPs [54, 55]. The flexible hydrophilic PEG chains sterically shield the active particle core, making it thermodynamically unfavourable for adsorption of proteins and reducing their uptake by surrounding immune cells [56]. In addition, alveolar macrophages show increased phagocytic uptake of particles > 250 nm [57]. Thereby, PEGylated DNA NPs that show superior colloidal stability (with lower aggregation) are less susceptible to rapid macrophage phagocytosis [58].

The acute toxicity of the different gene vectors was assessed after a single administration by analysis of cell counts from BALF samples collected 24 h post administration (Fig. 6B). Cell counts give an indication of immune cell infiltration; a higher number of cells in the collected BALF indicates an increased host immune response. In parallel, histological analysis was conducted for microscopic observation of immune cell infiltration induced by the inhaled gene vectors (Fig. 6D). Although not significant, we observed an increase in the percentage of neutrophils in the BALF of mice that inhaled non-PEGylated and PEGylated DNA NP formulations (16 ± 4% and 15 ± 4%, respectively) compared to water (7 ± 6%) (Fig. 6C). In addition, we found that non-PEGylated complexes exhibited elevated neutrophil infiltration compared to the mice treated with water (control) (Fig. 6E). All lung gene vectors trigger a level of innate immune response due to the introduction of foreign particles [59], so we went on to further interrogate the safety profile of the gene carriers by quantitative analysis of pro-inflammatory cytokine levels in BALF. Both 0% PEG DNA NPs and 40% PEG DNA NPs exhibited statistically significant but marginal increase in the levels of TNF-α and IL-1β (Fig. S4) compared to water-treated controls. Interestingly we did not observe an extra anti-inflammatory effect by the incorporation of PEG corona on the complexes. Peptide-based systems have negligible inflammatory effect, in comparison to cationic-polymer and lipid-based systems; which we demonstrate for the GET peptide system. Many factors can impact the potential immunogenic properties of PEG coatings including dosage, PEG molecular weight and PEG surface density [54]. Taken collectively, these data show that both PEGylated and non-PEGylated DNA NPs appear to elicit a very minimal inflammatory response following a single dose administration to healthy mouse lungs which is a property intrinsic to many peptide-based systems.

3. Conclusions

In recent years, overcoming the airway mucus barrier has been identified as one of the greatest challenges to successful respiratory gene therapy [16, 60]. Non-viral vectors can easily be modified to target specific cell-surface ligands, navigate extracellular barriers and improve intracellular trafficking of genetic cargo. Despite showing promise, the low transfection efficacy of non-viral vectors compared to viral gene carriers has limited their adoption. Importantly, GET-peptides (i.e. CPPs that have been modified for highly efficient intracellular uptake) have the potential to overcome challenges in insufficient gene transfer of non-viral vectors that have thus far inhibited their clinical application. In this study we have described a strategy for optimizing GET peptide vectors with an adaptable PEG coating to formulate DNA NPs with the desired characteristics for efficacious lung gene therapy. A critical challenge for modifying GET-technology for in vivo lung applications

was the balance between overcoming extracellular barriers without functionally masking the active peptide core which is required for GET-mediated enhanced cellular uptake. The conformational freedom afforded by flexible PEG chains and precisely tuning the density of PEG coating allowed for the selection of candidate formulations with desirable physiochemical properties. In addition, by using this method we were able to eliminate the need for employing a de-conjugation strategy for removal of PEG at the target site which often adds complexity to formulation and delivery processes. PEGylated particles were capable of maintaining colloidal stability in biological fluids and navigating efficiently through human CF sputum samples. When tested in mouse lung models in vivo these particles demonstrated superior lung distribution and transgene expression compared to the non-PEGylated version while retaining good safety profiles. Collectively these results show that GET peptides demonstrate significant potential for in vitro and in vivo gene transfer. Furthermore, PEG-GET technology could facilitate new approaches for overcoming biological barriers for the successful gene therapy of muco-obstructive lung diseases such as CF, asthma and chronic obstructive pulmonary disease (COPD).

4. Experimental section

4.1. Peptide synthesis

Peptides were synthesised using solid phase tert-butyloxycarbonyl (t-Boc) chemistry and purified to be > 90% by Protein Peptide Research Ltd. (PPR, UK). Peptide sequences are shown in Table S1. For the synthesis of PEGylated peptides, 5 kDa PEG chains were conjugated to FLR through a maleimide-thiol coupling reaction (PPR, UK). PEG maleimide was reacted with the thiol group of the terminal cysteine residue of the peptide. The PEG to peptide bond was formed through formation of a stable thioether linkage.

4.2. Preparation of DNA

For in vitro transfection, a Gaussia luciferase (GLuc) reporter plasmid (pCMV-Gluc2) containing a cytomegalovirus (CMV) promotor was employed (New England Biolabs). For multiple particle tracking and in vivo gene delivery, a firefly luciferase-expressing plasmid driven by a CMV promoter and fluorescently labelled versions of the plasmid DNA with Cyanine3 (Cy3) or Cyanine5 (Cy5) were prepared as previously described [21, 61]. Plasmid purity was confirmed using the NanoDrop 1000 spectrophotometer (ThermoFisher).

4.3. YO-PRO-1 assay for assessing DNA complexation

The optimal DNA binding ratio of peptide to DNA was determined using the YO-PRO-1 fluorescence-based assay. 10 μg DNA was diluted in 60 μL 4-(2-hydroxyethyl)-1-piperazineethanesulfonic acid (HEPES)-buffered saline (10 mM HEPES, 150 mM sodium chloride (NaCl) solution, pH 7.4). 1 mM YO-PRO-1 stock solution was diluted to 0.1 mM in dimethyl sulfoxide (DMSO). 2.7 μL of 0.1 mM YO-PRO-1 solution was made up to 60 μL in HEPES-buffered saline and added dropwise to the diluted DNA. The DNA/YO-PRO-1 solution was mixed, wrapped in foil and incubated for 5 h at room temperature (RT). Following incubation, the DNA/YO-PRO-1 solution was made up to 1 mL in HEPES-buffered saline and 100 μL aliquots were pipetted into Eppendorf tubes per treatment condition. Peptide amounts corresponding to the desired (+/−) charge ratios

(CRs) were added to each Eppendorf. Peptide/DNA/YO-PRO-1 solutions were mixed and incubated at RT for 10 min. Fluorescence measurements were analysed using the TECAN infinite 200PRO multimode reader. Similarly, a no DNA control was made by diluting 2.7 μL of the diluted YO-PRO-1 solution in 120 μL HEPES-buffered saline and following the procedure above.

4.4. Formation of DNA NPs

DNA NPs were formulated by the dropwise addition of DNA (0.1 μg/μL) to a volume of swirling 1 mM peptide solution. The peptide solution was a mixture of non-PEGylated and PEGylated peptide at 0%, 10%, 20%, 40%, 60%, 80% and 100% PEGylation rates. PEGylation rate was defined as the molar ratio of PEGylated to non-PEGylated peptide. Following the addition of DNA to peptide, the complexes were incubated for 30 min at RT. Polyethylenimine (PEI) NPs were made freshly as previously described [21]. NPs were washed three times with ultrapure distilled water and re-concentrated to 0.2 μg/μL using Amicon Ultra Centrifugal Filters (100,000 molecular weight cut-off; Millipore).

4.5. Dynamic light scattering (DLS) and zeta potential measurements

Hydrodynamic diameter of DNA NPs was determined in water by dynamic light scattering (DLS) and assessed in disposable low volume cuvettes. Zeta potential was measured in 10 mM NaCl at pH 7.0 by laser Doppler anemometry. NPs were measured by DLS following 1 h incubation in ultrapure water or 10% (v/v) bronchoalveolar lavage fluid (BALF) in phosphate buffered saline (PBS). Measurements of hydrodynamic size and zeta-potential were performed at RT using Zetasizer Nano ZS90 apparatus (Malvern Instruments). For each sample, 3 measurements were taken and each measurement was set to 10 runs.

4.6. DNase protection assay

Nuclease stability of DNA NPs was investigated following their incubation for 30 min at 37 °C in the presence of different concentrations of DNase I. DNase I buffer was made-up at 0.025 U/μL, 0.0025 U/μL and 0.00025 U/μL as described in the manufacturers guide (RNase-Free DNase, Qiagen). Following DNase treatment, complexes and naked pDNA were treated with proteinase K (20 μg) to remove peptide and allow visualisation of DNA by a gel sift assay. Samples were run on a 1% agarose gel (with 0.5 μg/mL ethidium bromide (EtBr)) in 1× trisacetate-ethylenediaminetetraacetic acid (EDTA) (TAE) buffer and visualized on a Luminescent Image Analyser LAS-4000 (FUJIFILM).

4.7. Cell culture of BEAS2B-R1 cells

BEAS2B-R1 human bronchial epithelial cells were maintained in growth media (GM) containing Dulbecco's modified Eagle's medium (DMEM) with 10% (v/v) fetal calf serum (FCS) supplemented with 2mM L-glutamine and 100 μg/mL streptomycin. All cells were incubated at 37 °C under humidified 5% carbon dioxide (CO_2) conditions, grown in T-75 culture flasks and passaged (with a standard trypsinization protocol using 0.25% (w/v) trypsin/2 mM EDTA solution) every 2–3 days or when they reached 80% confluency.

4.8. Cellular uptake of fluorescently-labelled DNA NPs

Cells were seeded at 4×10^4 cells/well in 24 well plates and incubated overnight in 500 μL of GM. For each well of cells to be treated, 1 μg rhodamine-labelled DNA was diluted in 25 μL Opti-MEM and mixed. Peptide in 25 μL Opti-MEM was added to the diluted DNA at CR3. The solution was mixed and incubated for 20 min at RT to allow complexation of the peptide to the DNA. The cells were aspirated, washed with PBS and replaced with 200 μL GM. Each well of cells was treated with 50 μL of peptide/DNA complex solution and incubated. Following a 4 h treatment, cells were treated with 25% (w/v) trypsin/2 mM EDTA and fixed in 3.7% (w/v) paraformaldehyde (PFA) in preparation for flow cytometry. Rhodamine-labelled cells were analysed on a Beckman Coulter Astrios EQ Cell Sorter using a green 561 nm laser (40,000 cells; gated on untreated cells by forward/side scatter). Data was analysed on flow cytometry analysis software (WEASEL) and mean fluorescence intensity was used for statistical analysis.

4.9. In vitro transfection of a luciferase reporter gene

Cells were seeded at 4×10^4 cells/well in 24 well plates and incubated overnight in 500 μL of GM. For each well of cells to be transfected, 1 μg DNA was diluted in 25 μL Opti-MEM and mixed. Peptide in 25 μL Opti-MEM was added to the diluted DNA at CR3. The solution was mixed and incubated for 20 min at RT to allow complexation of the peptide to the DNA. The wells were aspirated, washed with PBS and replaced with 200 μL GM. Each well of cells was treated with 50 μL of peptide/DNA complex solution. Following treatment, cells were incubated for 48 h at 37 °C under humidified 5% CO_2 conditions. GLuc expression was analysed as described in BioLux GLuc Assay Kit (New England Biolabs) and luminescence was measured in duplicate using a TECAN infinite 200PRO multimode reader.

The toxicity of gene carriers was assessed 48 h post-transfection by a PrestoBlue metabolic activity assay (Invitrogen). 10× solution of PrestoBlue reagent was diluted to a 1× solution in Hanks' balanced salt solution (HBSS). Cells cultured on 24 well plates were aspirated and washed with PBS. 250 μL 1× PrestoBlue reagent solution was added to each well, the plate was covered in foil (PrestoBlue assay is a light sensitive assay) and incubated at 37 °C for 15 min. Following incubation, 100 μL of PrestoBlue solution was transferred to a black 96 well plate. Fluorescence intensity was measured in duplicate using a TECAN infinite 200PRO multimode reader at excitation/emission 560 nm/590 nm. Relative fluorescence units (RFU) values of treated cells were divided by the fluorescence values of untreated cells for percentage cell viability.

4.10. Transmission electron microscopy (TEM)

DNA NPs were imaged using TEM to determine their morphology. The complexes were prepared as described above and diluted to 0.1 μg/μL in ultrapure water. A drop of the sample was cast onto a TEM grid and air-dried at RT for several hours before examination. The TEM (H7600; Hitachi High Technologies America, Johns Hopkins University USA) was operated at 80 kV and 3–5 images were taken per grid.

4.11. Multiple particle tracking

The diffusion of Cy3 and Cy5-labelled DNA NPs were tracked in freshly expectorated CF mucus of patients from Johns Hopkins Cystic Fibrosis Centre as previously described [9]. CF sputum samples were collected after receiving written informed consent and approval from the Johns Hopkins Institutional Review Board (study NA_00046768). There were no specific exclusion criteria for patients based on their clinical status. However, patient samples could be excluded based on quality (i.e. noticeable amounts of saliva contamination).

A blend of non-PEGylated and PEGylated FLR peptides were complexed with Cy3 or Cy5-labelled DNA (DNA concentration 0.5 μg/μL). 0.75 μL of fluorescently labelled complexes were added to 30 μL of a CF sputum sample and mixed. Sputum aliquots were used on the day of collection and kept sealed to prevent dehydration of the sample. Following a 1 h incubation at RT, 20 s movies of NP displacement were captured using an inverted epifluorescence microscope (Axio Observer; Zeiss). NP trajectories were analysed using multiple particle tracking (MTP) software based on a previously developed algorithm [44]. The algorithm was written on Matrix Laboratory (MATLAB) software and used to calculate the time-averaged mean squared displacement (MSD) of particles through the sputum. Particles were distinguished from background by fluorescence intensity, size, and eccentricity parameters, as previously demonstrated, and their trajectories were retrieved by monitoring x- and y-coordinates of complexes over time (i.e. frame). NP trajectories were then analysed using MTP software based on a previously developed algorithm which was used to calculate the ensemblemedian MSD of particles moving through the sputum [44]. For each sputum sample, 3–5 videos were collected.

5. Animal studies

Animal studies were carried out on 6–8 week female BALB/c mice as previously described [21] in accordance with Johns Hopkins University Animal Care and Use Committee guidelines.

Mice were anesthetized with an intraperitoneal (i.p.) injection of 2,2,2-tribromoethanol working solution (Sigma Aldrich). 50 μL FLR peptide/DNA NPs (DNA concentration 0.2 μg/μL) were administered by intratracheal microspray (Penn-Century). For bio-distribution studies, mice were treated with Cy3-labelled DNA NPs. Thirty min post administration, lungs were harvested and flash frozen in Optimal Cutting Temperature (OCT) compound (Fisher Healthcare). To determine biodistribution, lung slices were cryosectioned (CM1950 cryostat, Leica Biosystems) and stained with 4′,6-diamidino-2-phenylindole (DAPI). Images were taken on Carl Zeiss LSM-710 confocal microscope and quantified using ImageJ software (> 30 sections were analysed per mouse).

For transgene expression studies, mice were treated with luciferase expressing reporter plasmid driven by CMV promotor. 48 h post administration lungs were harvested and homogenised. The luciferase activity was measured using a luciferase assay kit (Thermo Scientific Pierce). Briefly, samples were freeze thawed 3 times in the presence of 1× reporter lysis buffer and centrifuged (10,000 × *g*, 10 min). 20 μL of supernatant was mixed with the

luciferase substrate and relative light units (RLU) were immediately measured on 20/20n luminometer. Bicinchoninic acid (BCA) Protein Assay Kit (Thermo Scientific Pierce) was used to normalise luciferase activity.

For the safety study, mice were treated with 0% or 40% PEGylated DNA NPs. 24 h post administration lungs were washed with 2.5 mL PBS × 3 to collect BALF for total cell counts and differential cell counts (Differential Quick Stain Kit, Modified Giemsa). Alternatively, lungs were fixed in paraffin, sectioned (CM1950 cryostat, Leica Biosystems) and stained with haematoxylin and eosin. Inflammatory scores were calculated by enumerating neutrophil infiltration, as previously described [62, 63]. Morphometric analysis was carried out double-blind in 10 random fields of view per slide and then summed (≥ 5 slides per mouse). Tissue slices were imaged on Carl Zeiss LSM-710 confocal microscope.

6. Statistical analysis

For in vitro transfection and uptake, data were compiled from six individual experiments (n = 6). The number of experiments (n) refers to experiments carried out on cells at different numbers of cell culture passages. For MPT experiments, median and SD were compiled from human CF patient mucus samples. Due to the heterogeneity of sputum samples, particles were tracked in n = 5/6 patient samples (3–5 videos/sample, > 100 DNA NPs tracked/sample). For in vivo biodistribution and transgene expression experiments, data were compiled from n = 3 (> 30 sections/mouse) and n = 8–9 mice/group, respectively. For total cell counts and differential cell counts in BALF, data were compiled from n = 8 and n = 5 (> 4 slides/mouse, > 100 cells were counted/slide) mice/group, respectively. For histopathological scores, data were compiled from n = 5 mice/group (≥ 5 slides/mouse, 10 random fields of view/slide). Data were presented as mean ± SD and analysed by Prism statistical analysis software (GraphPad). Statistical significance was measured between two groups using a two-tailed Student's t-test for comparison, between multiple groups by analysis of variance (ANOVA) with Bonferroni's multiple comparison test for post-hoc analysis or using ANOVA with Dunnett's test for the comparison of each treatment group with the control (for cell viability).

Supplementary Material

Refer to Web version on PubMed Central for supplementary material.

Acknowledgments

The research leading to these results has received funding from the European Research Council under the European Community's Seventh Framework Programme (FP7/2007-2013)/ERC grant agreement 227845. K.M.S. and J.E.D. acknowledge the support of the Medical Research Council, the Engineering and Physical Sciences Research Council, and the Biotechnology and Biological Sciences Research Council UK Regenerative Medicine Platform Hub "Acellular Approaches for Therapeutic Delivery" (MR/K026682/1). J.H. and J.S.S. acknowledge the support of the National Institute of Health (R01HL136617, R01HL127413, P30EY001765) and the Cystic Fibrosis Foundation (SUK18I0). A.L.T. acknowledges the support of Asthma UK and the Medical Research Foundation for her personal fellowship (MRFAUK- 2015-312).

References

[1]. Mehta A, The how (and why) of disease registers, Early Hum. Dev 86 (11) (2010) 723–728. [PubMed: 20833486]

[2]. Belkin RA, et al. , Risk factors for death of patients with cystic fibrosis awaiting lung transplantation, Am. J. Respir. Crit. Care Med 173 (6) (2006) 659–666. [PubMed: 16387803]

[3]. Griesenbach U, Pytel KM, Alton E, Cystic fibrosis gene therapy in the UK and elsewhere, Hum. Gene Ther 26 (5) (2015) 266–275. [PubMed: 25838137]

[4]. Rowe SM, Miller S, Sorscher EJ, Mechanisms of disease: cystic fibrosis, N. Engl. J. Med 352 (19) (2005) 1992–2001. [PubMed: 15888700]

[5]. Trapnell BC, et al. , Expression of the cystic-fibrosis transmembrane conductance regulator gene in the respiratory-tract of normal individuals and individuals with cystic-fibrosis, Proc. Natl. Acad. Sci. U. S. A 88 (15) (1991) 6565–6569. [PubMed: 1713683]

[6]. Grubb BR, et al. , Inefficient gene-transfer by adenovirus vector to cystic-fibrosis airway epithelia of mice and humans, Nature 371 (6500) (1994) 802–806. [PubMed: 7523956]

[7]. Wagner JA, et al. , A phase II, double-blind, randomized, placebo-controlled clinical trial of tgAAVCF using maxillary sinus delivery in patients with cystic fibrosis with antrostomies, Hum. Gene Ther 13 (11) (2002) 1349–1359. [PubMed: 12162817]

[8]. Konstan MW, et al. , Compacted DNA nanoparticles administered to the nasal mucosa of cystic fibrosis subjects are safe and demonstrate partial to complete cystic fibrosis transmembrane regulator reconstitution, Hum. Gene Ther 15 (12) (2004) 1255–1269. [PubMed: 15684701]

[9]. Schuster BS, et al. , Overcoming the cystic fibrosis sputum barrier to leading adeno-associated virus gene therapy vectors, Mol. Ther 22 (8) (2014) 1484–1493. [PubMed: 24869933]

[10]. Alton E, et al. , Repeated nebulisation of non-viral CFTR gene therapy in patients with cystic fibrosis: a randomised, double-blind, placebo-controlled, phase 2b trial, Lancet Respir. Med 3 (9) (2015) 684–691. [PubMed: 26149841]

[11]. Alton E, et al. , Preparation for a first-in-man lentivirus trial in patients with cystic fibrosis, Thorax 72 (2) (2017) 137–147. [PubMed: 27852956]

[12]. Jones AM, Helm JM, Emerging treatments in cystic fibrosis, Drugs 69 (14) (2009) 1903–1910. [PubMed: 19747007]

[13]. Sanders NN, et al. , Cystic fibrosis sputum - a barrier to the transport of nanospheres, Am. J. Respir. Crit. Care Med 162 (5) (2000) 1905–1911. [PubMed: 11069833]

[14]. Rubin BK, Mucus structure and properties in cystic fibrosis, Paediatr. Respir. Rev 8 (1) (2007) 4–7. [PubMed: 17419972]

[15]. Duncan GA, et al. , The mucus barrier to inhaled gene therapy, Mol. Ther 24 (12) (2016) 2043–2053. [PubMed: 27646604]

[16]. Kim N, et al. , Barriers to inhaled gene therapy of obstructive lung diseases: a review, J. Control. Release 240 (2016) 465–488. [PubMed: 27196742]

[17]. Ensign LM, et al. , Mucus penetrating nanoparticles: biophysical tool and method of drug and gene delivery, Adv. Mater 24 (28) (2012) 3887–3894. [PubMed: 22988559]

[18]. Turecek PL, et al. , PEGylation of biopharmaceuticals: a review of chemistry and nonclinical safety information of approved drugs, J. Pharm. Sci 105 (2) (2016) 460–475. [PubMed: 26869412]

[19]. Suk JS, et al. , Lung gene therapy with highly compacted DNA nanoparticles that overcome the mucus barrier, J. Control. Release 178 (2014) 8–17. [PubMed: 24440664]

[20]. Craparo EF, et al. , Pegylated polyaspartamide-polylactide-based nanoparticles penetrating cystic fibrosis artificial mucus, Biomacromolecules 17 (3) (2016) 767–777. [PubMed: 26866983]

[21]. Mastorakos P, et al. , Highly compacted biodegradable DNA nanoparticles capable of overcoming the mucus barrier for inhaled lung gene therapy, Proc. Natl. Acad. Sci. U. S. A 112 (28) (2015) 8720–8725. [PubMed: 26124127]

[22]. Dixon JE, et al. , Highly efficient delivery of functional cargoes by the synergistic effect of GAG binding motifs and cell-penetrating peptides, Proc. Natl. Acad. Sci. U. S. A 113 (3) (2016) E291–E299. [PubMed: 26733682]

[23]. Eltaher HM, et al. , Highly efficient intracellular transduction in three-dimensional gradients for programming cell fate, Acta Biomater. 41 (2016) 181–192. [PubMed: 27265151]

[24]. Thiagarajan L, Abu-Awwad HA-DM, Dixon JE, Osteogenic programming of human mesenchymal stem cells with highly efficient intracellular delivery of RUNX2, Stem Cells Transl. Med 6 (12) (2017) 2146–2159. [PubMed: 29090533]

[25]. Abu-Awwad HAM, Thiagarajan L, Dixon JE, Controlled release of GAG-binding enhanced transduction (GET) peptides for sustained and highly efficient intracellular delivery, Acta Biomater. 57 (2017) 225–237. [PubMed: 28457961]

[26]. Lee JY, et al. , Characterization of the surface immobilized synthetic heparin binding domain derived from human fibroblast growth factor-2 and its effect on osteoblast differentiation, J. Biomed. Mater. Res. A 83A (4) (2007) 970–979.

[27]. Santos JL, et al. , Non-viral gene delivery to mesenchymal stem cells: methods, strategies and application in bone tissue engineering and regeneration, Curr. Gene Ther 11 (1) (2011) 46–57. [PubMed: 21182464]

[28]. Luan L, et al. , Peptide amphiphiles with multifunctional fragments promoting cellular uptake and endosomal escape as efficient gene vectors, J. Mater. Chem. B 3 (6) (2015) 1068–1078. [PubMed: 32261985]

[29]. Marie D, Vaulot D, Partensky F, Application of the novel nucleic acid dyes YOYO- 1, YO-PRO-1, and PicoGreen for flow cytometric analysis of marine prokaryotes, Appl. Environ. Microbiol 62 (5) (1996) 1649–1655. [PubMed: 8633863]

[30]. Petty JT, Bordelon JA, Robertson ME, Thermodynamic characterization of the association of cyanine dyes with DNA, J. Phys. Chem. B 104 (30) (2000) 7221–7227.

[31]. Shen BQ, et al. , Conjugation site modulates the in vivo stability and therapeutic activity of antibody-drug conjugates, Nat. Biotechnol. 30 (2) (2012) 184–189. [PubMed: 22267010]

[32]. Wattiez R, Falmagne P, Proteomics of bronchoalveolar lavage fluid, J. Chromatogr. B 815 (1–2) (2005) 169–178.

[33]. Wheelock CE, et al. , Application of ‘omics technologies to biomarker discovery in inflammatory lung diseases, Eur. Respir. J 42 (3) (2013) 802–825. [PubMed: 23397306]

[34]. Khandare J, Minko T, Polymer-drug conjugates: Progress in polymeric prodrugs, Prog. Polym. Sci 31 (4) (2006) 359–397.

[35]. Zhang GD, et al. , Influence of anchoring ligands and particle size on the colloidal stability and in vivo biodistribution of polyethylene glycol-coated gold nanoparticles in tumor-xenografted mice, Biomaterials 30 (10) (2009) 1928–1936. [PubMed: 19131103]

[36]. Kleemann E, et al. , Nano-carriers for DNA delivery to the lung based upon a TAT-derived peptide covalently coupled to PEG-PEI, J. Control. Release 109 (1–3) (2005) 299–316. [PubMed: 16298009]

[37]. Hatakeyama H, Akita H, Harashima H, A multifunctional envelope type nano device (MEND) for gene delivery to tumours based on the EPR effect: a strategy for overcoming the PEG dilemma, Adv. Drug Deliv. Rev 63 (3) (2011) 152–160. [PubMed: 20840859]

[38]. Hatakeyama H, Akita H, Harashima H, The Polyethyleneglycol dilemma: advantage and disadvantage of PEGylation of liposomes for systemic genes and nucleic acids delivery to tumors, Biol. Pharm. Bull 36 (6) (2013) 892–899. [PubMed: 23727912]

[39]. Mishra S, Webster P, Davis ME, PEGylation significantly affects cellular uptake and intracellular trafficking of non-viral gene delivery particles, Eur. J. Cell Biol 83 (3) (2004) 97–111. [PubMed: 15202568]

[40]. Suh J, et al. , PEGylation of nanoparticles improves their cytoplasmic transport, Int. J. Nanomedicine 2 (4) (2007) 735–741. [PubMed: 18203439]

[41]. Miteva M, et al. , Tuning PEGylation of mixed micelles to overcome intracellular and systemic siRNA delivery barriers, Biomaterials 38 (2015) 97–107. [PubMed: 25453977]

[42]. Tatler AL, et al. , Caffeine inhibits TGFβ activation in epithelial cells, interrupts fibroblast responses to TGFβ, and reduces established fibrosis in *ex vivo* precision-cut lung slices, Thorax 71 (6) (2016) 565–567. [PubMed: 26911575]

[43]. Nassimi M, et al. , A toxicological evaluation of inhaled solid lipid nanoparticles used as a potential drug delivery system for the lung, Eur. J. Pharm. Biopharm 75 (2) (2010) 107–116. [PubMed: 20206256]

[44]. Schuster BS, et al. , Particle tracking in drug and gene delivery research: state-of-the-art applications and methods, Adv. Drug Deliv. Rev 91 (2015) 70–91. [PubMed: 25858664]

[45]. Fahy JV, Dickey BF, Medical progress airway mucus function and dysfunction, N. Engl. J. Med 363 (23) (2010) 2233–2247. [PubMed: 21121836]

[46]. Sheridan C, Gene therapy finds its niche, Nat. Biotechnol 29 (2) (2011) 121–128. [PubMed: 21301435]

[47]. Griesenbach U, Alton E, Moving forward: cystic fibrosis gene therapy, Hum. Mol. Genet 22 (2013) R52–R58. [PubMed: 23918661]

[48]. Ernst N, et al. , Interaction of liposomal and polycationic transfection complexes with pulmonary surfactant, J. Gene Med 1 (5) (1999) 331–340. [PubMed: 10738550]

[49]. Rudolph C, et al. , In vivo gene delivery to the lung using polyethylenimine and fractured polyamidoamine dendrimers, J. Gene Med 2 (4) (2000) 269–278. [PubMed: 10953918]

[50]. Davies LA, et al. , Enhanced lung gene expression after aerosol delivery of concentrated pDNA/PEI complexes, Mol. Ther 16 (7) (2008) 1283–1290. [PubMed: 18500249]

[51]. Walkey CD, et al. , Nanoparticle size and surface chemistry determine serum protein adsorption and macrophage uptake, J. Am. Chem. Soc 134 (4) (2012) 2139–2147. [PubMed: 22191645]

[52]. Lee BH, et al. , Adenoviral vectors stimulate innate immune responses in macrophages through cross-talk with epithelial cells, Immunol. Lett 134 (1) (2010) 93–102. [PubMed: 20850478]

[53]. Zhao DM, et al. , Heparin rescues sepsis-associated acute lung injury and lethality through the suppression of inflammatory responses, Inflammation 35 (6) (2012) 1825–1832. [PubMed: 22782595]

[54]. Gref R, et al. , ‘Stealth’ corona-core nanoparticles surface modified by polyethylene glycol (PEG): influences of the corona (PEG chain length and surface density) and of the core composition on phagocytic uptake and plasma protein adsorption, Colloid. Surf. B Biointerf 18 (3–4) (2000) 301–313.

[55]. Jokerst JV, et al. , Nanoparticle PEGylation for imaging and therapy, Nanomedicine 6 (4) (2011) 715–728. [PubMed: 21718180]

[56]. Vonarbourg A, et al. , Parameters influencing the stealthiness of colloidal drug delivery systems, Biomaterials 27 (24) (2006) 4356–4373. [PubMed: 16650890]

[57]. Weisman RA, Korn ED, Phagocytosis of latex beads by acanthamoeba. I. biochemical properties, Biochemistry 6 (2) (1967) 485. [PubMed: 4860149]

[58]. Chono S, et al. , Influence of particle size on drug delivery to rat alveolar macrophages following pulmonary administration of ciprofloxacin incorporated into liposomes, J. Drug Target 14 (8) (2006) 557–566. [PubMed: 17043040]

[59]. Ferrari S, et al. , Immunological hurdles to lung gene therapy, Clin. Exp. Immunol 132 (1) (2003) 1–8. [PubMed: 12653829]

[60]. Sanders N, et al. , Extracellular barriers in respiratory gene therapy, Adv. Drug Deliv. Rev 61 (2) (2009) 115–127. [PubMed: 19146894]

[61]. Suk JS, et al. , The penetration of fresh undiluted sputum expectorated by cystic fibrosis patients by non-adhesive polymer nanoparticles, Biomaterials 30 (13) (2009) 2591–2597. [PubMed: 19176245]

[62]. Kajon AE, Gigliotti AP, Harrod KS, Acute inflammatory response and remodeling of airway epithelium after subspecies B1 human adenovirus infection of the mouse lower respiratory tract, J. Med. Virol 71 (2) (2003) 233–244. [PubMed: 12938198]

[63]. da Silva AL, et al. , DNA nanoparticle-mediated thymulin gene therapy prevents airway remodeling in experimental allergic asthma, J. Control. Release 180 (2014) 125–133. [PubMed: 24556417]

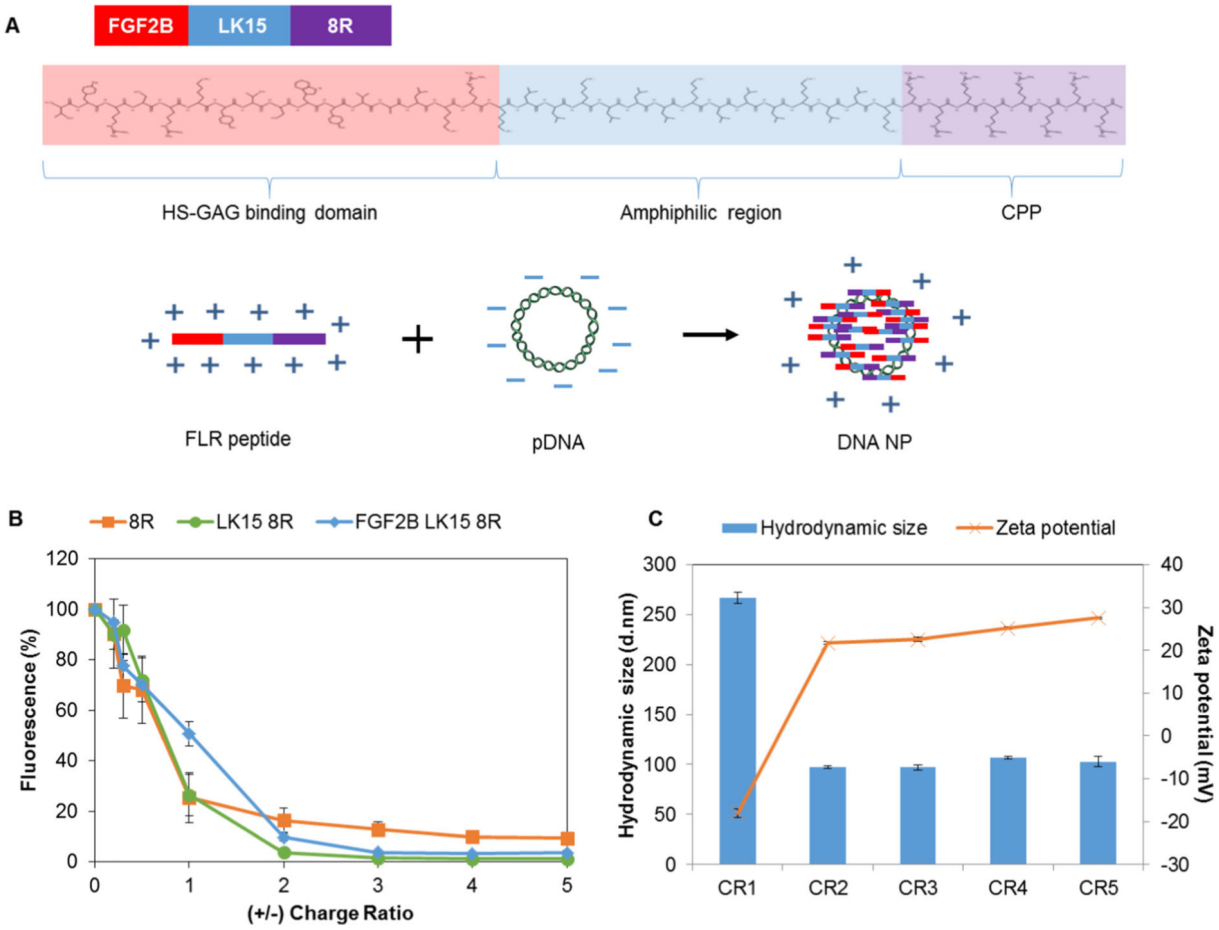

Fig. 1.

DNA NP formation and characterisation. (A) FLR is a multi-domain peptide made up of a HS GAG binding domain (red), amphiphilic region (blue) and CPP (purple). When mixed with DNA, FLR peptides form electrostatic interactions with the negatively charged phosphate groups of the plasmid to form nanoparticles (NPs) through self-assembly. (B) The ability of GET peptides to bind DNA was assessed using a YO-PRO1 fluorescence-based assay. The graph shows a decrease in the percentage fluorescence as the peptide out competes the dye by complexing DNA at different tested (+/−) charge ratios (CRs). (C) Following the formation of DNA NPs, the physiochemical characteristics of complexes were investigated at different CRs. Hydrodynamic size and zeta-potential were measured in ultrapure water and 10 mM NaCl at pH 7.0, respectively. Error bars indicate SD, $n = 3$. (For interpretation of the references to colour in this figure legend, the reader is referred to the web version of this article.)

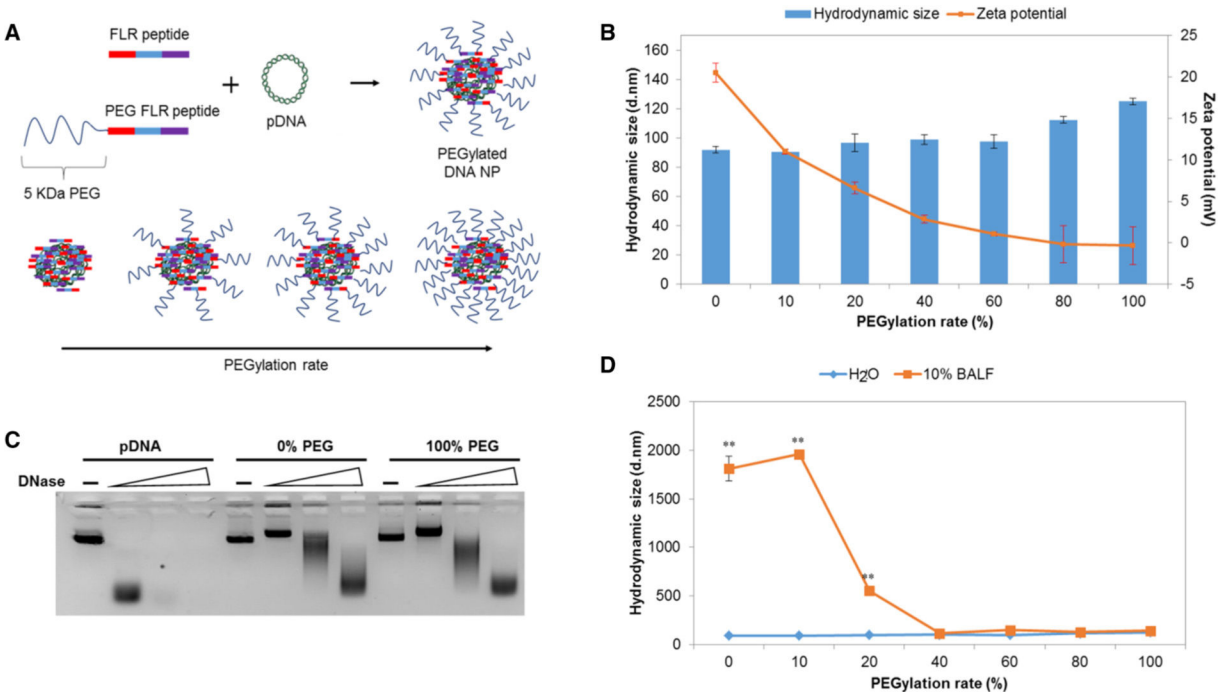

Fig. 2.

The effect of PEGylation on the physiochemical properties of DNA NPs. (A) Schematic of non-PEGylated and PEGylated FLR peptides blended at different molar ratios to form DNA NPs with a tuneable coating of PEG on the outer surface. We hypothesized that by varying the PEG component we were able to form DNA NPs at different PEGylation rates. For example 20% PEGylation rate would represent a mixture of 20% PEGylated peptide and 80% non-PEGylated peptide. (B) To confirm the formation of DNA NPs we measured the diameter and charge of complexes at 0%, 10%, 20%, 40%, 60%, 80% and 100% PEGylation rates. The hydrodynamic size and zeta-potentials were measured in ultrapure water and 10 mM NaCl at pH 7.0, respectively. (C) We tested the ability of complexes to protect DNA from nucleases. Naked pDNA, 0% PEG DNA NPs and 100% PEG DNA NPs were incubated with DNase I for 30 min, digested using proteinase K and visualized using a gel shift assay. Degradation of DNA was evidenced by a shift, smear or loss of the DNA band. (D) Stability of PEGylated DNA complexes was investigated following 1 h incubation in ultrapure water or 10% (*v*/v) BALF in PBS. Hydrodynamic diameter of respective NPs was measured by DLS. Error bars indicate SD, n = 3. Two-tailed Student's *t*-test, $*P < .05$, $**P < .01$.

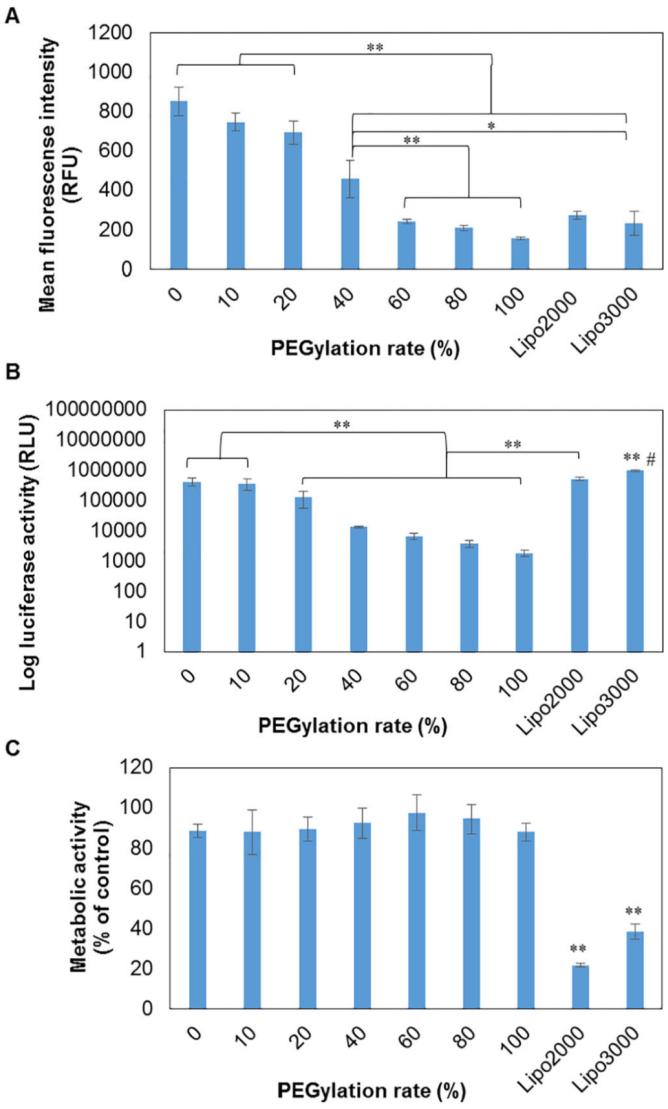

Fig. 3.

In vitro uptake and transfection efficiency of DNA NPs at different PEGylation rates. (A) Human bronchial epithelial cells (BEAS2B-R1) cells were treated with rhodamine-labelled DNA complexes for 4 h, trypsinized to remove any extracellularly bound DNA and fluorescence intensity was measured using flow cytometry. (B-C) For the transgene expression study, BEAS2B-R1 cells were transfected for 24 h with 1 μg of a reporter gene expressing luciferase. (B) Transfection efficiency and (C) cell viability (PrestoBlue assay) were assessed at a 48 h time-point. Error bars indicate SD, $n = 6$. One-way ANOVA with Bonferroni's post-test or one-way ANOVA with Dunnett's test for the comparison of each treatment group with the control (for cell viability), *P < .05, **P < .01.

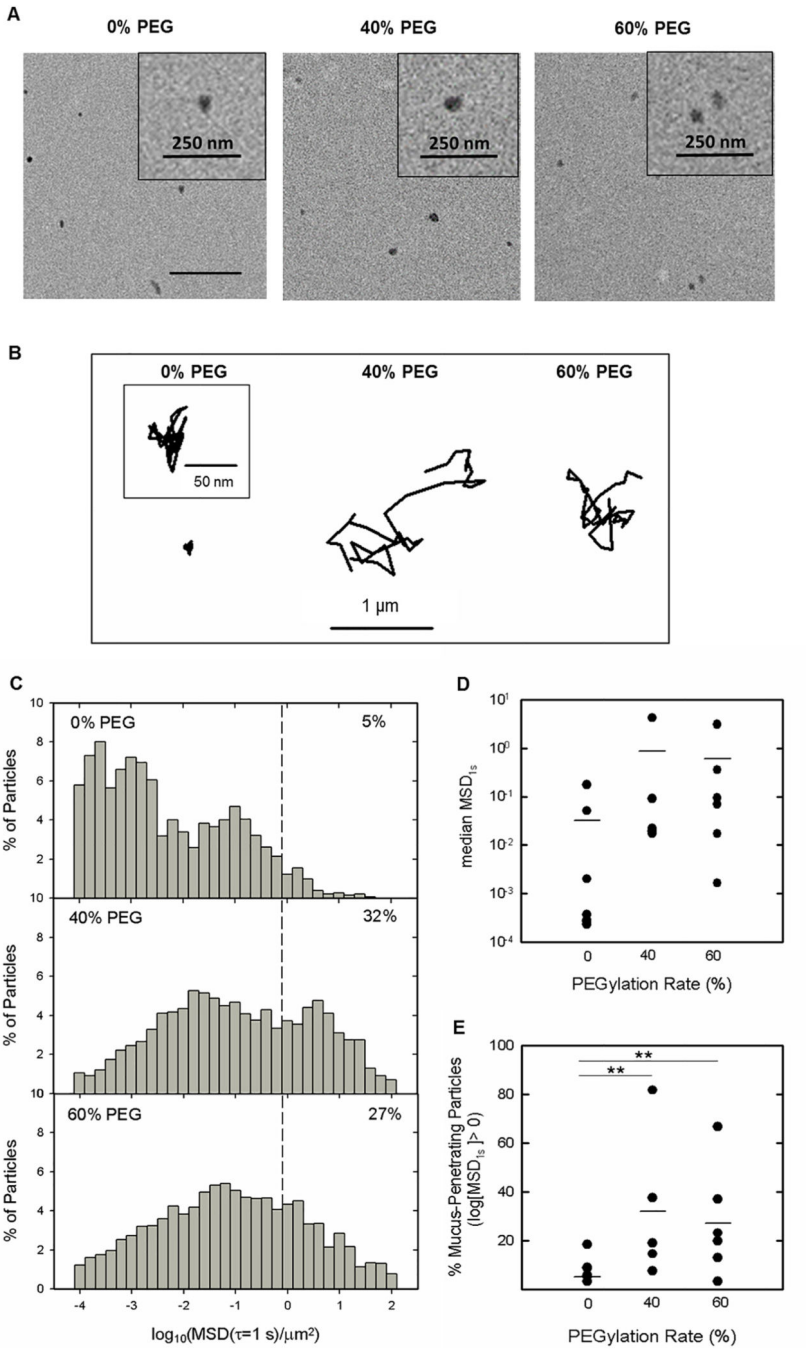

Fig. 4.

Multiple particle tracking of DNA NPs in ex vivo human CF sputum samples. The diffusion of DNA NPs at 0%, 40% and 60% PEGylation rates was investigated in freshly expectorated patient CF sputum samples. (A) Representative transmission electron micrographs of the respective NPs. Scale bar, 500 nm on original images and 250 nm on inserts. Following a 1 h incubation in sputum, movies of NP displacement were captured and analysed by MPT technology. (B) Representative trajectories of particles moving through CF sputum and (C) mean squared displacement (MSD) of particles. Dot plots of (D) ensemble-median MSD

and (E) percentage mucus penetrating particles (MSD ≥ 1 μm^2). Error bars indicate SD, n = 5–6 patient samples (> 100 DNA NPs tracked for each experiment). One-way ANOVA with Bonferroni's post-tests; *P < .05, ** P < .01.

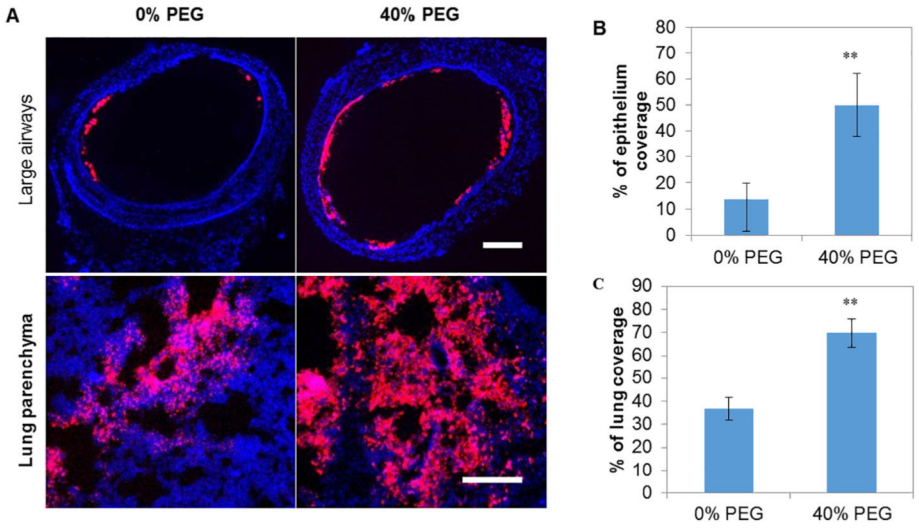

Fig. 5.

In vivo bio-distribution of PEGylated DNA complexes in healthy mouse lung models. Lung tissues were harvested 30 min following intratracheal administration of Cy5-labelled DNA NPs at 0% and 40% PEGylation rates. (A) Representative images of NP distribution in large airways and lung parenchyma following administration of the respective NPs (red). Scale bar, 0.2 mm. Cell nuclei were stained with DAPI (blue). Image-based quantification of (B) coverage of NPs in large airways and (C) distribution of NPs in the lung parenchyma. Error bars indicate SD, n = 3 mice/group (> 30 sections were analysed per mouse). Two-tailed Student's *t*-test, *P < .05, **P < .01. (For interpretation of the references to colour in this figure legend, the reader is referred to the web version of this article.)

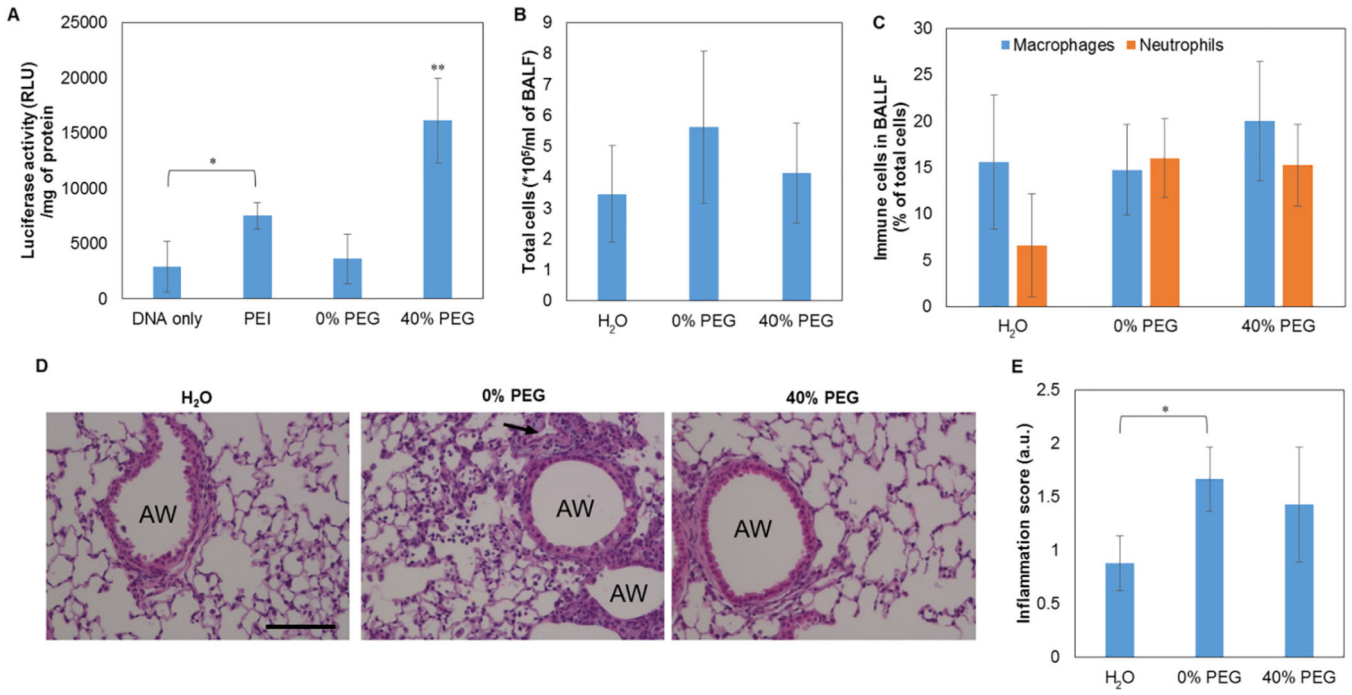

Fig. 6.

Transgene expression and safety profile of DNA NPs. (A) In vivo mouse lung transgene expression of luciferase activity following intratracheal administration of PEGylated DNA NPs. Acute toxicity of the complexes was assessed by (B) cell counts and (C) percentage of macrophages and neutrophils from BALF of treated lungs 24 h post administration. (D) Representative images of lung sections stained with haematoxylin and eosin. AW, airway, arrow indicates cellular infiltrate. Scale bar, 100 μm. (E) Histopathological scoring of lung inflammation. Error bars indicate SD, n = 8–9 mice/group for transgene expression and cell counts, n = 5 mice/group for histopathological scoring. One-way ANOVA with Bonferroni's post-tests; *P < .05, **P < .01.